PAPER • OPEN ACCESS

Conceptual design of the cryogenic system and estimation of the recirculated power for CFETR

To cite this article: Xiaogang Liu *et al* 2017 *Nucl. Fusion* **57** 016037

OPEN ACCESS
IOP Publishing | International Atomic Energy Agency
Nuclear Fusion
Nucl. Fusion **57** (2017) 016037 (9pp)
doi:10.1088/1741-4326/57/1/016037

Conceptual design of the cryogenic system and estimation of the recirculated power for CFETR

Xiaogang Liu[1], Lilong Qiu[1], Junjun Li[1], Zhaoliang Wang[1], Yong Ren[1], Xianwei Wang[2], Guoqiang Li[1], Xiang Gao[1] and Yanfang Bi[1]

[1] Institute of Plasma Physics, Chinese Academy of Sciences, Hefei 230031, People's Republic of China
[2] Jiang Su University of Technology, Changzhou 213001, People's Republic of China

E-mail: xgliu@ipp.ac.cn

Received 27 July 2016, revised 26 October 2016
Accepted for publication 4 November 2016
Published 8 December 2016

Abstract

The China Fusion Engineering Test Reactor (CFETR) is the next tokamak in China's roadmap for realizing commercial fusion energy. The CFETR cryogenic system is crucial to creating and maintaining operational conditions for its superconducting magnet system and thermal shields. The preliminary conceptual design of the CFETR cryogenic system has been carried out with reference to that of ITER. It will provide an average capacity of 75 to 80 kW at 4.5 K and a peak capacity of 1300 kW at 80 K. The electric power consumption of the cryogenic system is estimated to be 24 MW, and the gross building area is about 7000 m^2. The relationships among the auxiliary power consumed by the cryogenic system, the fusion power gain and the recirculated power of CFETR are discussed, with the suggestion that about 52% of the electric power produced by CFETR in phase II must be recirculated to run the fusion test reactor.

Keywords: CFETR, cryogenic system, superconducting magnet, heat load, cryoplant, cryodistribution, recirculated power

(Some figures may appear in colour only in the online journal)

1. Introduction

China is planning to construct the CFETR in the 2020s [1], in order to bridge the physical and engineering gaps between ITER and the fusion demonstration reactor (DEMO). The CFETR tokamak is envisioned to comprise two phases [2]: First, in phase I a long pulse or quasi-steady-state plasma operation with burn duty cycle up to 50%, fusion power $P_{fus} = 200$ MW, fusion power gain $Q = 3$ and tritium breeding ratio TBR > 1 will be demonstrated. Then, in Phase II the goal of CFETR will be realizing fusion energy production with $P_{fus} = 1000$ MW, $Q = 12$ and self-sustaining tritium production. The CFETR in Phase I is an ITER-like tokamak except for the additional tritium breeding blanket. The plasma current (10 MA), the major and minor radii ($R = 5.7$ m and $r = 1.6$ m), and the toroidal field (5.0 T) of CFETR are a little smaller than those of ITER.

The conceptual design and evaluation of CFETR as a fusion science facility have been conducted [2–4], and some R&D programs have been granted by the Ministry of Science and Technology of China, such as the project of developing the CFETR central solenoid model coil from 2014 to 2019 [5].

The cryogenic system is one of the most important auxiliary systems for CFETR, to create and maintain the low-temperature operating conditions for the superconducting magnets, cryopumps and other users. It consists of the cryoplant and the cryodistribution system. The cryoplant is composed of helium and nitrogen refrigerators combined with 80 K helium loops. The cryodistribution system will distribute the cooling power produced by the cryoplant, through a

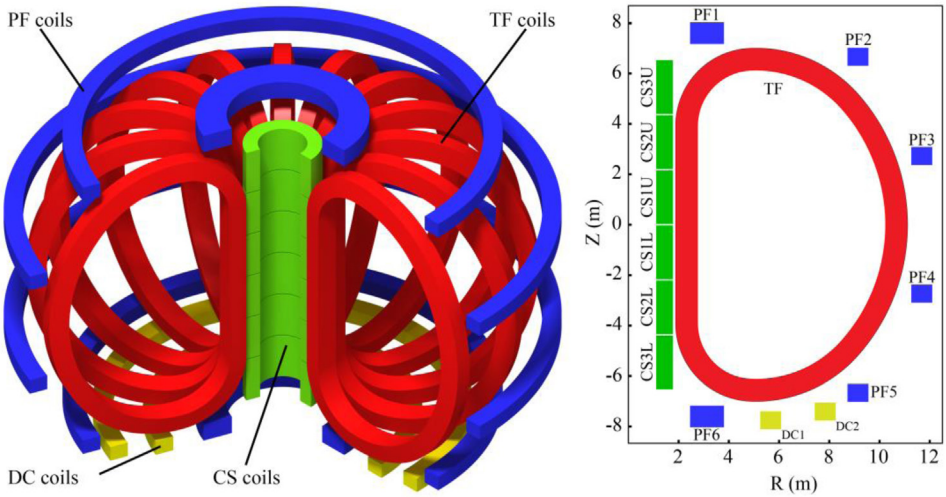

Figure 1. Overview of structure and cross-section distribution of the CFETR magnet system.

complex system of cryodistribution-lines and valve boxes, to the cryogenic components.

The helium refrigerators will produce cooling power to 4.5 K for the superconducting magnets, the magnet structures (mainly the TF coil cases and supporting structures), and the cryopumps. They will also provide 50 K helium gas (GHe) to cool the high temperature superconducting (HTS) current leads of the magnet system. The nitrogen refrigerators combined with 80 K loops will produce cooling power for the thermal shields and the pre-cooling of the helium refrigerators.

The key design requirement of the CFETR cryogenic system is to withstand the large pulsed heat loads deposited in the magnets due to the magnetic field variation and the neutron production from deuterium–tritium (D–T) fusion reaction [6–8].

The China National Integration Design Group is now focusing on the engineering conceptual design of CFETR, and the detailed heat load analysis of the magnet system has not been conducted yet. So, in this paper, we need to extrapolate the average heat loads of the CFETR cryogenic system from that of ITER.

The CFETR cryogenic system provides cooling power to the tokamak; at the same time it consumes some tens of MW of electric power. This electric power, which is one of the major parts used by the auxiliary systems, together with that consumed by the blanket cooling system and the additional heating system, constitute the so-called recirculated power. To some extent, the auxiliary power for the cryogenic system will influence the recirculated power and the fusion power gain [9], thereby affecting the feasibility of CFETR as a test reactor for electric power production.

This paper is organized as follows. First, the magnet system of CFETR is introduced and the cold mass is estimated. Next, the average heat load of the cryogenic system is extrapolated from that of ITER. Then, the conceptual design of the cryogenic system is presented. After that, the relationships among the auxiliary power consumed by the cryogenic system, the recirculated power and fusion power gain are studied. Finally, a conclusion is given.

2. The magnet system of CFETR

The core function of the CFETR cryogenic system is to maintain the low-temperature conditions for the superconducting magnet system, and furthermore, the magnet system is the largest cryogenic user [10]. Therefore, it is important to determine the dimension and weight of the CFETR magnet system.

The CFETR superconducting magnet system is composed of 16 toroidal field (TF) and six poloidal field (PF) coils, a central solenoid (CS) coil stacked with six modules and 12 correction coils (CC) [4]. The TF and CS coils operate at high magnetic field of ~12 T and are made of Nb_3Sn cable-in-conduit-conductor (CICC), while the PF and CC coils, operating at low field of ~6 T consist of NbTi CICC conductor [11]. The CFETR magnet system are placed in the cryostat and an 80 K GHe cooled thermal shield is used to reduce the radiation from room temperature. All the coils are actively cooled with forced flow supercritical helium (SHe) [12].

The structural overview and cross-sectional dimensions of the CFETR magnet system are shown in figure 1. Since CFETR in phase I is an ITER-like tokamak except for the additional breeding blanket, and all the coils (TF, PF, CS and CC) of CFETR share a similar design philosophy and use the same superconducting conductors as their ITER counterparts [13], the weight of the CFETR coils can be extrapolated from the corresponding ITER coils [14]. Comparing the volume of a TF winding pack (structure) of CFETR and one of ITER, their ratio is 1.07 (1.05). Therefore, the mass of a winding pack (structure) of 1/16 CFETR TF coils can be deduced to be 118.1 tons (265.3 t); thus the total mass of 16 TF coils of CFETR is 6135 t. The mass of the PF and CS coils can be estimated analogously. The main parameters of the CFETR TF, PF and CS coils are listed in table 1. The total cold mass of the CFETR magnet system is ~9235 t (10 135 t for ITER).

Table 1. Mass of the main magnet system of CFETR extrapolated from ITER.

	Magnet system	CFETR	ITER
TF coil	Number of WP	16	18
	WP volume (m^3)	18.77	17.56
	Coil case volume (m^3)	1.04	0.99
	WP mass (t)	118.12	110.50
	WP structure mass (t)	265.34	252.70
	Total mass (t)	6135.30	6537.60
PF coil	Number of WP	6	6
	WP total volume (m^3)	32.11	35.70
	Total mass (t)	1945.90	2163.00
CS coil	Number of Module	6	6
	Module total volume (m^3)	11.94	15.83
	Module mass (t)	499.54	662.70
	Total mass (t)	734.35	974.20
Total cold mass of the magnet system (t)		9235	10 135

3. Average heat loads of the CFETR cryogenic system

The heat loads of the CFETR cryogenic system are estimated based on the CFETR baseline scenario: a fusion power of 200 MW with plasma current of 10 MA and burn duty cycle (defined as the ratio of plasma burn time to repetition time) of 50%. The plasma burn time of CFETR baseline scenario will range from 10^4 s to 10^5 s, taking into account the burn time of 10^2 s–10^4 s for ITER and 10^7 s for DEMO.

Two ITER scenarios are considered to extrapolate the average heat loads of the CFETR cryogenic system [15]: (1) The 9 MA quasi-steady state scenario with fusion power of 360 MW, burn time of 2950 s and repetition time of 12000 s. (2) The 15 MA baseline scenario with fusion power of 500 MW, burn time of 400 s and repetition time of 1800 s.

The extrapolation of the main heat loads for the CFETR cryogenic system are displayed in table 2. They are classified to two temperature levels of 4.5 K and 80 K, and are listed in the following.

3.1. Nuclear heat

The nuclear heat due to the D–T neutron production during the plasma burn time is mainly deposited in the TF coils and the magnet structures; it is proportional to the fusion power. The nuclear heat during the plasma burn time can be extrapolated to be 5.90 kW for CFETR. Then a value of 2.95 kW is derived by averaging over the plasma repetition time, considering the burn duty cycle of 50%.

3.2. AC losses & eddy currents

The conductor AC losses and structure eddy current losses of the CFETR magnet system mainly exist during the plasma burn, because of the requirement to control the plasma. They are caused by the variation of the magnetic field and associated with the plasma current. The values are 32.45 kW and 35.18 kW for the two ITER scenarios, as we can see from table 2, so we can estimate it to be ~33 kW for the CFETR baseline scenario. Although the AC losses and eddy currents also exist in the plasma ramp up and down phase, this time is much shorter than the burn time for CFETR, therefore their contribution to the average load is negligible. Consequently, an average value of 16.5 kW can be obtained by applying the burn duty cycle of 50%.

3.3. Static heat load

The static heat load of the CFETR magnet system consists of the following five parts: (i) the thermal radiation of the cryostat and vacuum vessel; (ii) the thermal conduction of the TF coil gravity supports and thermal shield supports; (iii) the thermal radiation and conduction of the cryodistribution system; (iv) the cold end heat load of the HTS current leads; (v) the Ohmic heat of the TF coil joints (TF coils charged). As detailed in the above five parts, the static heat load is associated with the surface area and cold mass of the magnet system. Here the cold mass of the magnet system is used to scale the static heat load of CFETR, which is extrapolated to be 11.3 kW at 4.5 K.

3.4. Heat load of cryopumps

The cryopumps are used to remove ashes from the torus, and to keep the high vacuum of the cryostat and the neutral beam injectors. As a coarse approximation, the heat loads of the cryopumps could be considered to be proportional to the plasma volume Rr^2, where R and r are the major and minor radii respectively. For CFETR $Rr^2 = 14.6$, while it is 24.8 for ITER. In addition, the burn duty cycle of CFETR is 50%, which is 22.2% for the baseline scenario of ITER. The higher burn duty cycle will make the heat load of the cryopumps larger. Therefore, this part of heat load can be extrapolated to be 7.7 kW + 83 g s^{-1} LHe.

3.5. Heat load of cold compressors and SHe circulators

The heat loads of the magnets and cryopumps will be extracted by SHe circulators and then delivered to the helium plant via heat exchangers immersed in the LHe bath. A cold compressor is used to pump the LHe bath and to maintain the bath temperature below 4.5 K.

It can be considered that the heat load of cold compressors and SHe circulators is related to the total SHe flow rate of the magnets and cryopumps. This flow rate is associated with the heat loads of magnets and cryopumps. Note that the heat load of the magnets includes the static and dynamic (nuclear heat and AC losses & eddy currents) load. The heat load of the magnets and cryopumps can be added up to a total of 48.9 kW equivalent at 4.5 K for CFETR; the equiavalent figure is 48.7 kW for the ITER baseline scenario. Thus the heat load of cold compressors and SHe circulators is coarsely estimated to be 11.4 kW.

Table 2. Average heat loads of the CFETR cryogenic system and comparison with ITER.

		CFETR baseline scenario		ITER quasi-steady-state scenario		ITER baseline scenario	
		10MA–200 MW—steady state		9 MA–360 MW—12 000 s		15MA–500 MW—1800 s	
		Burn time/Repetition time = 50%		2950 s/12 000 s = 24.6%		400 s/1800 s = 22.2%	
Type of heat load	Temp. level	Burn	Average	Burn	Average	Burn	Average
Nuclear heat	4.2 K	5.90 kW	2.95 kW	10.62 kW	2.61 kW	14.40 kW	3.20 kW
AC losses & eddy currents	4.2 K	33.00 kW	16.50 kW	32.45 kW	8.96 kW	35.18 kW	17.29 kW
Static heat load (TF charged)	4.2 K	11.3 kW		12.4 kW			
Cryopumps and small users	4.5 K	7.7 kW + 83 g s^{-1} LHe		6.5 kW + 70 g s^{-1} LHe			
SHe circulators & cold compressors	4.2 K	11.4 kW		11.4 kW			
HTS current leads	50 K	147 g s^{-1} GHe		150 g s^{-1} GHe			
Total heat load of He plant	**4.5 K**	**64.6 kW**		**65 kW**			
Thermal Shields	80 K	757 kW		800 kW (Baking)			

Table 3. Main parameters of the HTS current lead for CFETR.

Coil	Number of pairs	Maximum current (kA)
TF coil	8	67.4
PF coil	6	53
CS coil	6	57
Correction coil	6	10

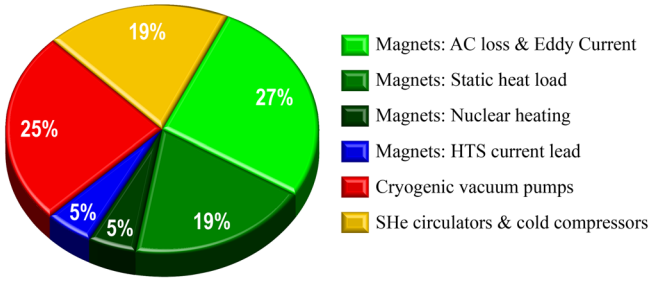

Figure 2. Main 4.5 K heat load distribution of CFETR cryogenic system.

3.6. Heat load of HTS current leads

The use of HTS current leads can greatly reduce the conduction heat load from room temperature. The number of HTS current leads needed for the CFETR magnet system and the corresponding maximum operating current are shown in table 3. With an approximate heat load of 0.058 g $s^{-1}kA^{-1}$ [16], the 50 K helium flow rate needed for the HTS current leads is 147 g s^{-1}.

3.7. Total 4.5 K equivalent load

In this section, we add up the aforementioned six loads to get the total equivalent 4.5 K heat load. Since these six contributions are in different temperatures and forms, now we investigate how to convert them equivalently to 4.5 K load.

Consider a refrigerator that moves heat Q_c from a cold reservoir with temperature T_c to an ambient temperature sink T_0 (assuming $T_0 = 300$ K), by consuming minimum mechanical work of W_{min}; the Carnot equation can be expressed as

$$W_{min} = T_0 \frac{Q_c}{T_c} - Q_c. \quad (1)$$

This equation can be written in a different form by introducing the entropy variation $\Delta S = Q_c/T_c$, and the enthalpy variation ΔH [17]:

$$W_{min} = T_0 \Delta S - \Delta H. \quad (2)$$

According to equation (1), to produce 1 W cooling power at 4.5 K and 4.2 K, a mechanical work of 65.67 W and 70.43 W is needed respectively. By comparing the required minimum mechanical work, the relation between the cooling power at 4.2 K and 4.5 K can be derived as 1 W @4.2 K ≈ 1.07 W @4.5 K.

According to equation (2), the minimum work needed to cool helium at 1 g s^{-1} from 300 K to 50 K with pressure of 4.0 bar [18] is 1 g s^{-1} × (300 K × 9.32 J $g^{-1}K^{-1}$ − 1229.13 J g^{-1}) = 1566.87 W. Thus, we can obtain 1 g s^{-1} He @50 K, 4 bar ≈ 23.86 W@4.5 K, which means 147 g s^{-1} GHe at 50 K is equivalent to ~3.5 kW at 4.5 K. This agrees well with the estimation in [19].

Similarly, the relation between the liquefaction of 1 g s^{-1} LHe (pressure of 1.3 bar) and the cooling power at 4.5 K can be derived by using equation (2): 1 g s^{-1} LHe @4.5 K, 1.3 bar ≈ 100 W@4.5 K [17].

Given the above equivalent relations, the estimated total 4.5 K equivalent load can be added up to 64.6 kW. The distribution of the heat load is illustrated in figure 2, from which we can see the heat load of the magnet system accounts for 56% of the overall 4.5 K load.

3.8. Heat load of thermal shields

Cooling power to 80 K is produced by the N_2 plant. Besides providing 80 K GHe to the thermal shields of the tokamak, the N_2 plant also supplies LN_2 to the precooling heat exchangers of the He refrigerators. Note that this precooling power is not

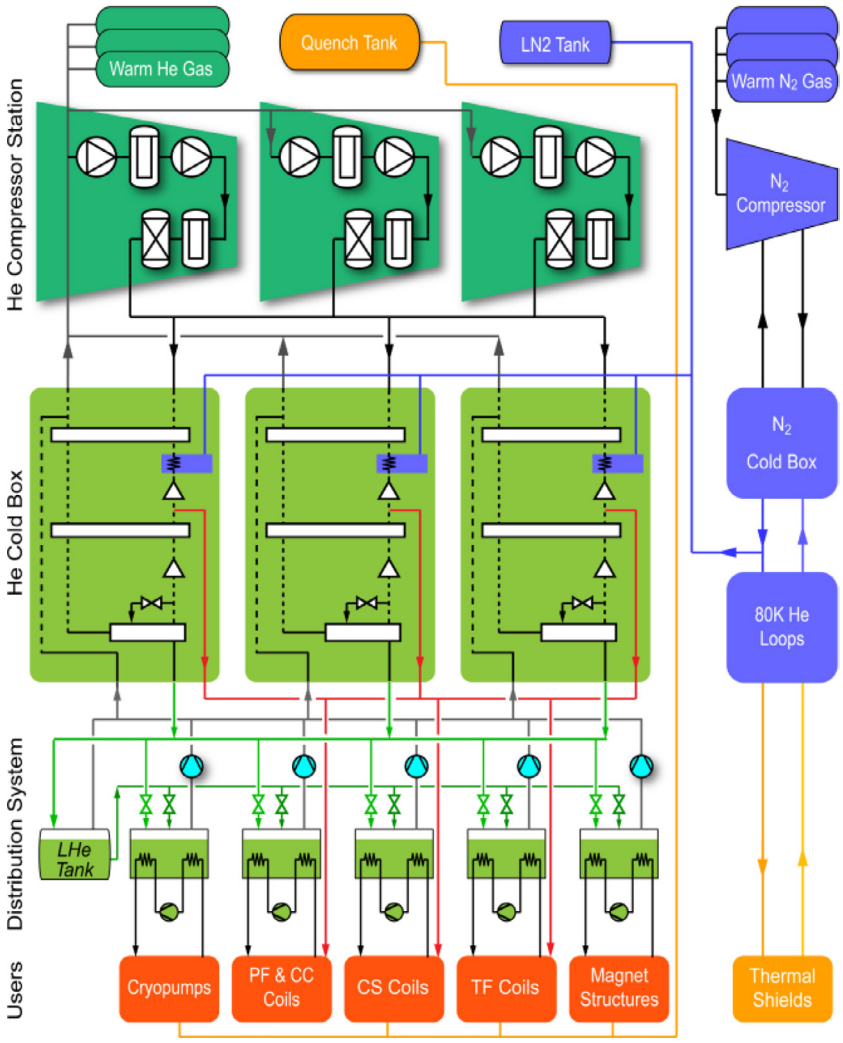

Figure 3. Principal process flow diagram of the CFETR cryogenic system.

a heat load on the cryogenic system, since the LN_2 precooling is actually an internal process of the cryogenic system [9].

For the thermal shields of the vacuum vessel and cryostat, the heat load is proportional to the thermal radiation surface and consequently to $(1 + k^2)Rr$ [19], where the plasma elongation k is 2 for CFETR. So this load is estimated to be 757 kW@80 K for CFETR, referring to the value of 800 kW for ITER.

4. Conceptual design of the CFETR cryogenic system

According to the estimation of average heat load at 4.5 K, a helium plant with an average refrigeration capacity within the range of 75–80 kW is required for CFETR. This capacity range refers to the installed capacity of the ITER helium plant, which is 75 kW [20] to withstand an average heat load of 65 kW.

As for the N_2 plant, in order to cooperate with the He plant and to cool the thermal shields, a maximum equivalent capacity of ~1300 kW is needed [20].

The principal process flow diagram for the CFETR cryogenic system is presented in figure 3. Cooling power at different temperature levels of 4.2 K, 4.5 K, 50 K, and 80 K will be produced and delivered to the users [21]. Taking into account the design experience of the ITER helium plant [22], the helium plant of CFETR cryogenic system is divided into three helium refrigerators. These will operate in parallel with liquid nitrogen precooling, which is provided by the nitrogen plant. The nitrogen cryoplant consists of two N_2 liquefiers operating in parallel.

The schematic layout of the CFETR cryogenic system is illustrated in figure 4, the gross building area is about 7000 m^2 [23, 24].

Normally, the cryogenic system will supply SHe to the superconducting coils with an inlet temperature of 4.2 K–4.5 K. The temperature in this range provides an appropriate temperature margin for both the Nb_3Sn conductor to operate at ~12 T and the NbTi conductor at ~6 T.

However, for any one of the coils, the inlet temperature of the SHe can be further lowered to 3.8 K to accommodate conductor and physics requirements [25], and to allow the capability of withstanding possible operation faults or design/analysis errors [14]. For example, as reported in [26], due to the calculated nuclear heat load during the 400 s burning being drastically increased from 14.4 kW to 28.4 kW, an

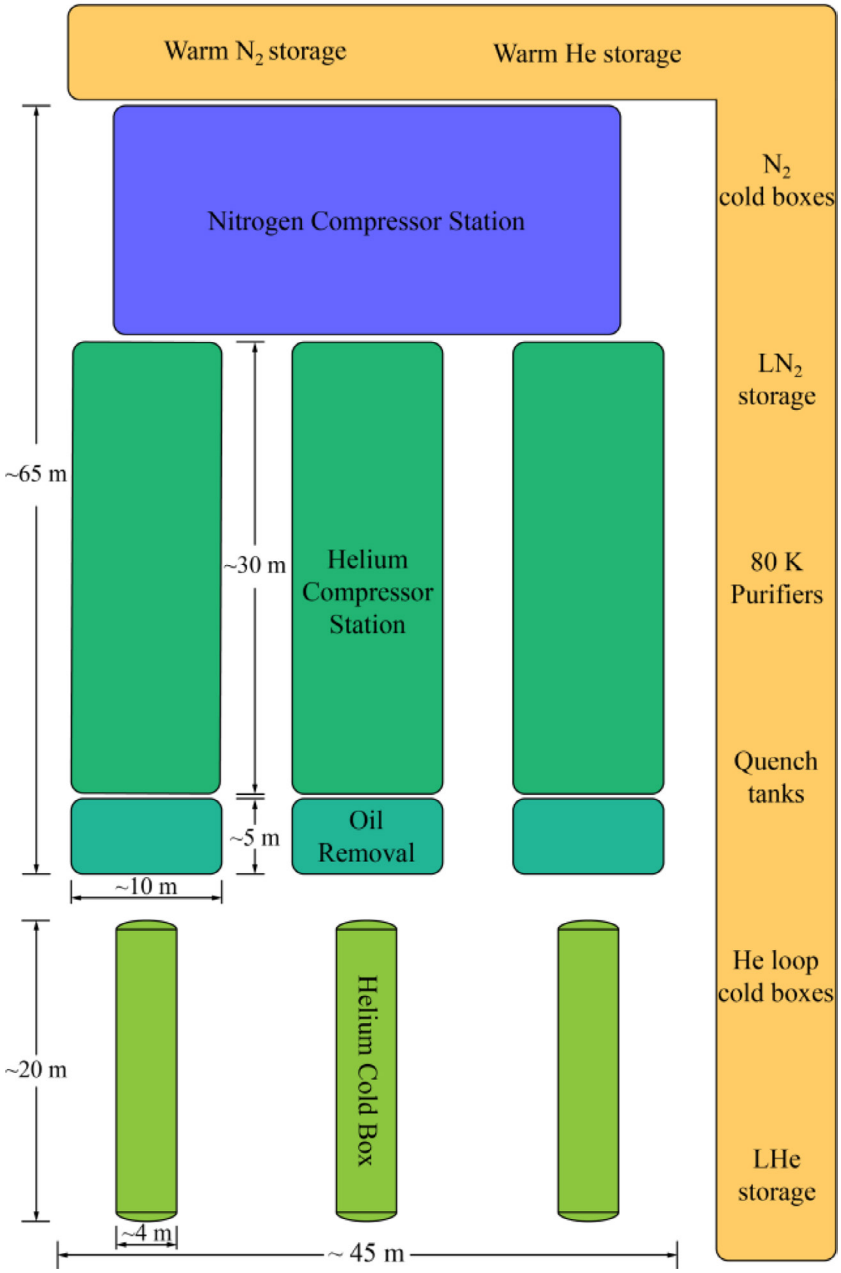

Figure 4. Schematic layout of the CFETR cryogenic system.

optimization of the ITER cryodistribution system is proposed to cool the TF and PF&CC to 3.8 K. This optimization is adopted as shown in the distribution system of figure 3; by individually controlling the bath temperature with a dedicated cold compressor for each of the LHe baths, enhanced cooling at 3.8 K can be concentrated to any one of the coils in need.

To mitigate the large pulsed heat loads deposited in the magnets due to magnetic field variation and neutron production, different approaches could be considered [27]. One way is to use the helium storage in the LHe tank during the plasma burning phase [28]. Another way is to temporarily bypass the heat exchanger of the magnet structures, thereby making use of its high thermal inertia. Then, during the plasma dwell time before the next shot, the normal operating temperature of the structures can be recovered. Moreover, the operation speed of the SHe circulators can be varied to mitigate the pulsed loads.

Table 4. Electric power consumed by CFETR cryogenic system.

Temperature level	4.5 K	80 K
Cooling power	64.6 kW	757 kW
Overall efficiency	1/250	1/10
Electric power	16.2 MW	7.6 MW

The overall efficiency of a cryoplant is the ratio between the cooling power produced and the electric power consumed. For the CFETR cryogenic system, an overall efficiency of 1/250

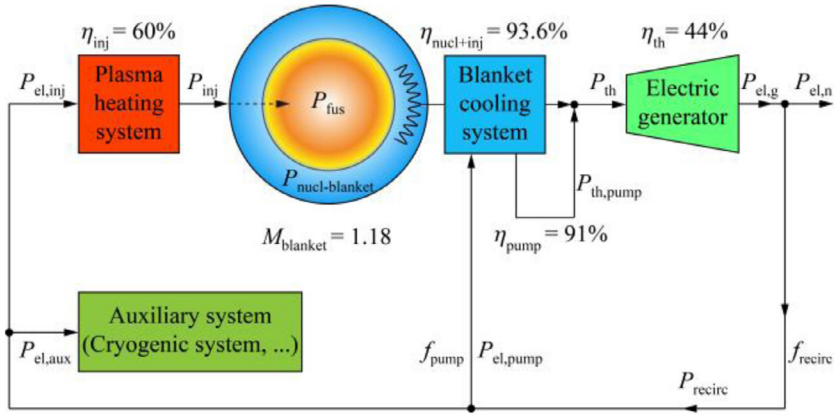

Figure 5. Schematic process flow diagram of the power flux in CFETR.

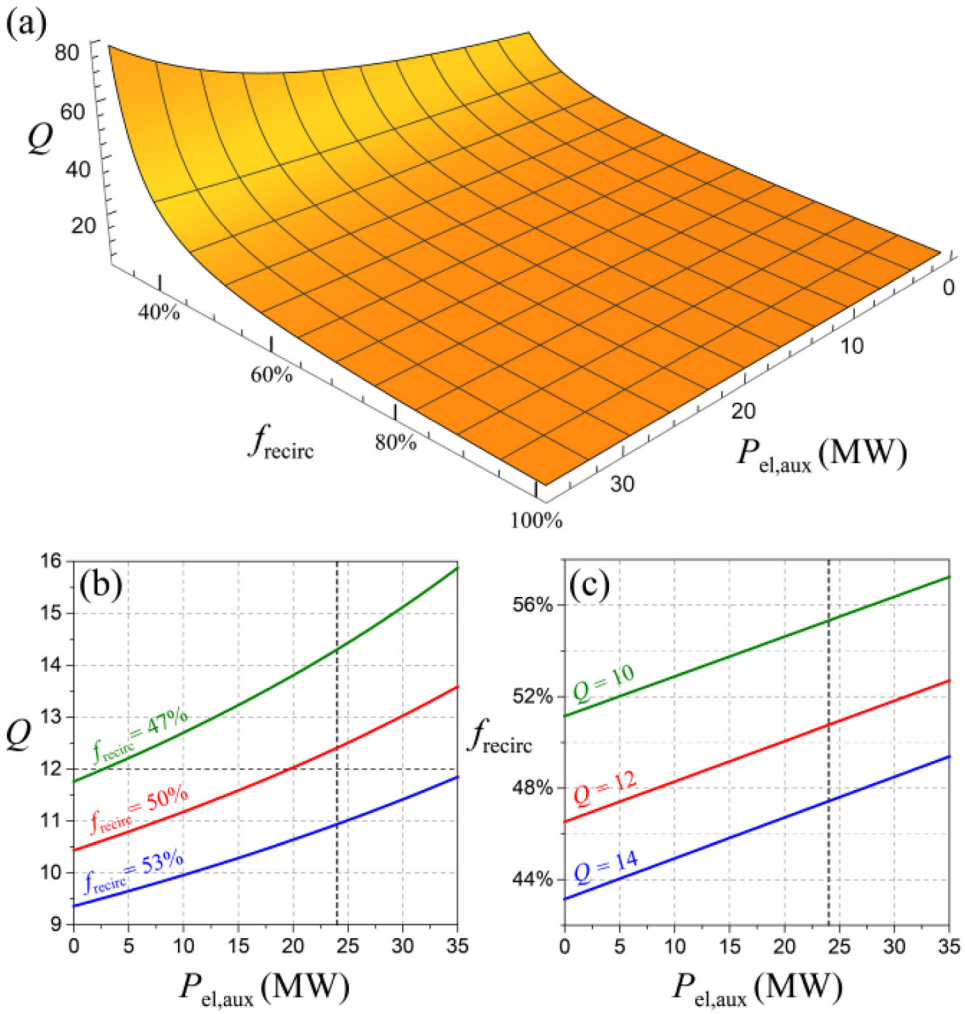

Figure 6. (*a*) Fusion power gain Q as a function of the recirculated fraction f_{recirc} and auxiliary electric power $P_{el,aux}$. (*b*) The Q and (*c*) f_{recirc} as a function of $P_{el,aux}$.

and 1/10 [19] is assumed for the helium plant and the nitrogen plant respectively, based on the measured performance of the LHC cryogenic system [29, 30]. The efficiency of large scale helium refrigerators at 4.5 K ranges from ~1/220 to ~1/300 [31]. For the CFETR helium plant, in order to realize the goal of 1/250, helium turbines with high efficiency need to be employed, which is to say ~80% (75%) for turbines working above (below) 20 K.

The resulting electric power required by the CFETR cryogenic system is shown in table 4.

5. Relationships among the auxiliary power consumed by the cryogenic system, the fusion power gain, and the recirculated power

A schematic process flow diagram of the power flux [32] in CFETR is shown in figure 5. In a fusion reactor, the fusion power gain Q may be defined as the ratio of the fusion power P_{fus} to the injected heating power P_{inj}, P_{inj} is the power required to maintain the high temperature of the plasma. The fraction f_{recirc} of the gross electrical output $P_{\mathrm{el,g}}$ produced by the power plant, expressed here as P_{recirc}, is recirculated to run the reactor. A part of this recirculated power, designated as $P_{\mathrm{el,pump}}$, is used to energize the blanket cooling system. In this cooling process, the fusion heat is absorbed and then converted into useful thermal power P_{th} for electricity generation. Another part, $P_{\mathrm{el,inj}}$, is dedicated to the plasma heating system to deliver additional heating power to the plasma. And the last part, $P_{\mathrm{el,aux}}$, is utilized to run the auxiliary system—this is mainly consumed by the cryogenic system.

In the following, we will discuss the relationships among the fusion power gain Q, the recirculated fraction f_{recirc} and the auxiliary electric power $P_{\mathrm{el,aux}}$ of CFETR. The following expressions [32] can be obtained through figure 5:

$$P_{\mathrm{el,g}} = \frac{1 + f_{\mathrm{neut}}\,(M_{\mathrm{blanket}} - 1) + \frac{1}{Q}}{1 - \eta_{\mathrm{th}}\, f_{\mathrm{pump}}\, \eta_{\mathrm{pump}}}\, \eta_{\mathrm{th}} \eta_{\mathrm{nucl+inj}}\, P_{\mathrm{fus}} \qquad (3)$$

$$f_{\mathrm{recirc}} = f_{\mathrm{pump}} + \frac{P_{\mathrm{fus}}}{Q\ \eta_{\mathrm{inj}}}\,\frac{1}{P_{\mathrm{el,g}}} + \frac{P_{\mathrm{el,aux}}}{P_{\mathrm{el,g}}}, \qquad (4)$$

where $f_{\mathrm{neut}} = 0.8$ is the fraction of the fusion power taken by the neutrons in a D–T reaction, and the following parameters are quoted from the European DEMO-2007 project [33]: $\eta_{\mathrm{inj}} = 0.6$ is the efficiency of the additional heating, $M_{\mathrm{blanket}} = 1.18$ is the energy gain of the blanket neutron multiplication, $\eta_{\mathrm{nucl+inj}} = 93.6\%$ is the efficiency with which $P_{\mathrm{fus}} + P_{\mathrm{nucl-blanket}} + P_{\mathrm{inj}}$ is converted into useful heat, $\eta_{\mathrm{th}} = 44\%$ is the thermodynamic efficiency of the electric power generation, $f_{\mathrm{pump}} = 21.4\%$ is the fraction of the gross electric power $P_{\mathrm{el,g}}$ to run the blanket cooling system, and $\eta_{\mathrm{pump}} = 91\%$ is the fraction of pumping power $P_{\mathrm{el,pump}}$ converted into useful heat.

According to equations (3) and (4), and considering $P_{\mathrm{fus}} = 1000$ MW in the phase II of CFETR, the relation among Q, f_{recirc} and $P_{\mathrm{el,aux}}$ can be derived, which is plotted in figure 6. We observe from figure 6(*a*) that if f_{recirc} goes lower than ~40%, the required Q for CFETR must be drastically increased to balance the reactor.

It is evaluated that $Q = 12$ is realizable for CFETR in phase II [2]; the electric power needed for the cryogenic system of CFETR in phase I is 24 MW, so $P_{\mathrm{el,aux}}$ in phase II should be larger than 24 MW. Note that in [19], for a typical DEMO, the electric power for the cryogenic system is estimated to be 27 MW.

As we can see from figures 6(*b*) and (*c*), when $Q = 12$ and $P_{\mathrm{el,aux}} > 24$ MW, the recirculated power fraction f_{recirc} should be about 52%. Therefore, supposing $Q = 12$ and $f_{\mathrm{recirc}} = 52\%$, the net electric power produced by CFETR in phase II will be about 266 MW, and the recirculated power will be about 288 MW.

6. Conclusion

The heat load estimation and preliminary conceptual design of the CFETR cryogenic system is presented in this study. Besides, the relationships among the fusion power gain, the recirculated power and the auxiliary electric power in CFETR are discussed. This study could be a starting point for the future design of the CFETR cryogenic system.

Acknowledgments

This work is supported in part by the National Magnetic Confinement Fusion Science Program of China (Grant No. 2014GB105002), the National Natural Science Foundation of China (Grant No. 51406215, 51306195 and 51407178), the Anhui Provincial Natural Science Foundation (Grant No. 1408085QE90), and in part by the Science Foundation within the Institute of Plasma Physics, Chinese Academy of Sciences, under Grant No. Y45ETY2305. The authors greatly appreciate the helpful discussion with Dr Lu Xiaofei.

References

[1] Li J. 2015 Closing gaps to CFETR readiness *IAEA TCM 3rd DEMO Workshop (Hefei, China, 11–14 May 2015)* www-naweb.iaea.org/napc/physics/meetings/TM49530/website/talks/May%2012%20Sessions/Li_J.pdf
[2] Chan V. *et al* 2015 *Nucl. Fusion* **55** 023017
[3] Wan B. *et al* 2014 *IEEE Trans. Plasma Sci.* **42** 495–502
[4] Song Y.T. *et al* 2014 *IEEE Trans. Plasma Sci.* **42** 503–9
[5] Liu X. *et al* 2016 *IEEE Trans. Plasma Sci.* **44** 1559–63
[6] Richard L.S. *et al* 2013 *Cryogenics* **57** 173–80
[7] Claudet G. *et al* 2001 *Fusion Eng. Des.* **58–9** 205–9
[8] Chang H.S. *et al* 2012 *IEEE Trans. Appl. Super. Cond.* **22** 4703804
[9] Duchateau J. *et al* 2006 *Nucl. Fusion* **46** S94–9
[10] Kalinin V. *et al* 2006 *Fusion Eng. Des.* **81** 2589–95
[11] Ren Y. *et al* 2015 *Nucl. Fusion* **55** 093002
[12] Hoa C. *et al* 2012 *AIP Conf. Proc.* **1434** 1943–50
[13] Sborchia C. *et al* 2014 *Nucl. Fusion* **54** 013006
[14] Mitchell N. *et al* 2012 *IEEE Trans. Appl. Super. Cond.* **22** 4200809
[15] Mitchell N. 2010 Magnet heat loads for cryoplant design *ITER Organization Internal Document 2MASMT v1.7* https://user.iter.org/?uid=2MASMT
[16] ITER 2006 Design Description Document-Magnet-Engineering Description *ITER Organization Internal Document 22HV5L v2.2* https://industryportal.f4e.europa.eu/IP_WS_DOCUMENTS_TMP/16/_F4E-OPE-086_[6]%20Design%20Description%20Document%20(DDD)%20DDD11-1%20Engineering%20Description.pdf
[17] Lebrun P. 2007 An introduction to cryogenics *Accelerator Technology Department Report (CERN, Geneva, Switzerland)* http://inspirehep.net/record/751195/files/at-2007-001.pdf
[18] Ballarino A. *et al* 2015 *IOP Conf. Series: Mat. Sci. and Eng.* **101** 012119
[19] Duchateau J. *et al* 2014 *Fusion Eng. and Des.* **89** 2606–20
[20] Monneret E. *et al* 2015 *Phys. Proc.* **67** 35–41

[21] Serio L. *et al* 2010 *AIP Conf. Proc.* **1218** 651–62
[22] Henry D. *et al* 2010 *AIP Conf. Proc.* **1218** 676–83
[23] Fauvea E. *et al* 2014 ITER LHe plants—Parallel Operation *ICEC-2014 (Enschede, The Netherlands, 7–11 July 2014)* https://indico.cern.ch/event/244641/contributions/1563427/attachments/418365/581026/O4-2_ERIC_FAUVE-TUE-AF-O4.pdf
[24] Lamaison V. *et al* 2014 *AIP Conf. Proc.* **1573** 337–44
[25] Serio L. 2009 *Fusion Sci. Technol.* **56** 672–5
[26] Chang H.S. *et al* 2016 *IEEE Trans. Appl. Supercond.* **26** 4203704
[27] Chang H. S. *et al* 2012 *AIP Conf. Proc.* **1434** 1691–8
[28] Fauvea E. *et al* 2014 *Phys. Proc.* **67** 42–7
[29] Dauguet P. *et al* 2008 *AIP Conf. Proc.* **985** 557–63
[30] Barth K. 2006 Operation of cryogenic for CERN experiments and LHC test facilities *Workshop on Cryogenic Operations (Stanford, California, 9–11 May 2006)* www.slac.stanford.edu/econf/C0605091/present/BARTH.PDF
[31] Gruehagen H. and Wagner U. 2004 Measured performance of four new 18 kW@4.5 K helium refrigerators for the LHC cryogenic system *Proc. 20th Int. Cryogenic Eng. Conf. (Beijing, China, 11–14 May 2004)* http://cds.cern.ch/record/795005/files/lhc-project-report-796.pdf?version=1&origin=publication_detail
[32] Johner J. 2011 *Fusion Sci. Technol.* **59** 308–49 www.ans.org/pubs/journals/fst/a_11650
[33] Li-Puma A. *et al* 2009 *Fusion Eng. and Des.* **84** 1197–205